

UCLA

UCLA Previously Published Works

Title

Environmental Impacts by Fragments Released from Nanoenabled Products: A Multiassay, Multimaterial Exploration by the SUN Approach.

Permalink

<https://escholarship.org/uc/item/46q4d7wz>

Journal

Environmental science & technology, 52(3)

ISSN

0013-936X

Authors

Amorim, Mónica JB
Lin, Sijie
Schlich, Karsten
[et al.](#)

Publication Date

2018-02-01

DOI

10.1021/acs.est.7b04122

Peer reviewed

Environmental Impacts by Fragments Released from Nanoenabled Products: A Multiassay, Multimaterial Exploration by the SUN Approach

Mónica J.B. Amorim,[†] Sijie Lin,^{‡,§} Karsten Schlich,^{||} José M. Navas,[⊥] Andrea Brunelli,[#] Nicole Neubauer,[○] Klaus Vilsmeier,[○] Anna L. Costa,[∇] Andreas Gondikas,[¶] Tian Xia,[§] Liliana Galbis,[⊥] Elena Badetti,[#] Antonio Marcomini,[#] Danail Hristozov,[#] Frank von der Kammer,[¶] Kerstin Hund-Rinke,^{||} Janeck J. Scott-Fordsmand,[▲] André Nel,[§] and Wendel Wohlleben^{○,◆,*}

[†]Department of Biology and CESAM, University of Aveiro, 3810-193, Aveiro, Portugal

[‡]College of Environmental Science and Engineering, State Key Laboratory of Pollution Control and Resource Reuse, Tongji University, Shanghai 200092, China

[§]Division of NanoMedicine, Department of Medicine, Center for Environmental Implications of Nanotechnology, California NanoSystems Institute, University of California, Los Angeles, California 90095, United States

^{||}Department of Ecotoxicology, Fraunhofer Institute for Molecular Biology and Applied Ecology, Auf dem Aberg 1, 57392 Schmallenberg, Germany

[⊥]Department of Environment, Instituto Nacional de Investigación y Tecnología Agraria y Alimentaria (INIA), Centra De la Coruña Km 7.5, E-28040 Madrid, Spain

[#]Department of Environmental Sciences, Informatics and Statistics (DAIS), University Ca' Foscari of Venice, Via Torino 155, 30170 Venice Mestre, Italy

[∇]National Research Council of Italy, Institute of Science and Technology for Ceramics (CNR-ISTEC), Via Granarolo, 64, I-48018 Faenza, Italy

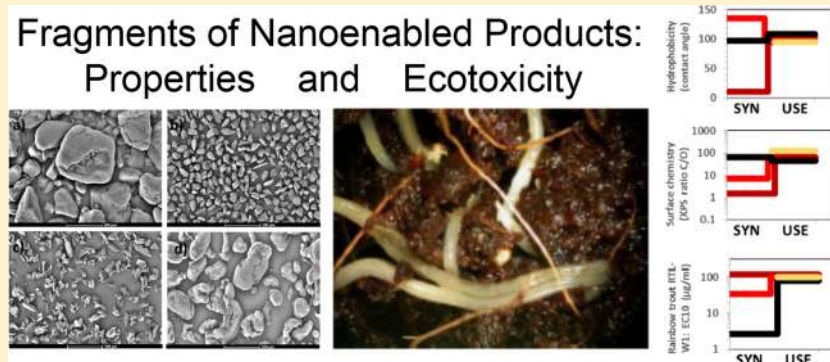
[○]Department of Material Physics, BASF SE, Carl-Bosch-Strasse 38, 67056 Ludwigshafen, Germany

[◆]Department of Experimental Toxicology and Ecology, BASF SE, D-67056 Ludwigshafen, Germany

[¶]Department of Environmental Geosciences, University of Vienna, 1090 Vienna, Austria

[▲]Department of Bioscience, Aarhus University, Vejlsovej 25, PO Box 314, 8600 Silkeborg, Denmark

Supporting Information



ABSTRACT: Nanoenabled products (NEPs) have numerous outdoor uses in construction, transportation or consumer scenarios, and there is evidence that their fragments are released in the environment at low rates. We hypothesized that the lower surface availability of NEPs fragment reduced their environmental effects with respect to pristine nanomaterials. This hypothesis was explored by testing fragments generated by intentional micronisation (“the SUN approach”; Nowack et al. Meeting the Needs for Released Nanomaterials Required for Further Testing: The SUN Approach. *Environmental Science & Technology*, 2016 (50), 2747).
continued...

Received: August 17, 2017

Revised: December 15, 2017

Accepted: December 22, 2017

Published: January 27, 2018

The NEPs were composed of four matrices (epoxy, polyolefin, polyoxymethylene, and cement) with up to 5% content of three nanomaterials (carbon nanotubes, iron oxide, and organic pigment). Regardless of the type of nanomaterial or matrix used, it was observed that nanomaterials were only partially exposed at the NEP fragment surface, indicating that mostly the intrinsic and extrinsic properties of the matrix drove the NEP fragment toxicity. Ecotoxicity in multiple assays was done covering relevant media from terrestrial to aquatic, including sewage treatment plant (biological activity), soil worms (*Enchytraeus crypticus*), and fish (zebrafish embryo and larvae and trout cell lines). We designed the studies to explore the possible modulation of ecotoxicity by nanomaterial additives in plastics/polymer/cement, finding none. The results support NEPs grouping by the matrix material regarding ecotoxicological effect during the use phase. Furthermore, control results on nanomaterial-free polymer fragments representing microplastic had no significant adverse effects up to the highest concentration tested.

■ INTRODUCTION

Nanocomposites are a dominant class of nanoenabled products (NEPs), and in particular, those with a “durable” matrix, such as rubber, cements, plastics, and coatings, are often utilized in outdoor use.^{1,2} Processes such as wear, tear, manufacturing and shredding (mechanical processes) and photolysis, hydrolysis, aggressive use environments, and thermal decomposition (chemical processes) contribute to the degradation of nanocomposites^{3,4} and induce releases into the environment at various time scales along the lifecycle.^{5,6} Pristine engineered nanomaterials (ENM) can induce adverse effects on environmental species in aquatic, sediment, and soil compartments.⁷ This is relevant for emission scenarios such as spills during the ENM synthesis phase of the lifecycle but not for the NEP use phase. For NEPs made of chemically resilient nanocomposite materials, the only relevant case for NEP outdoor use, nanocomposite fragments of the NEPs are the dominant physical–chemical form of environmental releases during the use phase.^{8–10} However, to the best of our knowledge, no study has ever reported on environmental effects by NEP fragments. This is a serious gap in environmental risk assessment of nanomaterials. NEP fragments differ from pristine ENM in key physical–chemical properties such as composition, size, surface chemistry.¹¹ Their environmental release rates on the order of grams per year¹² are too low to measure their properties and environmental effects directly for degrading NEPs, which in a controlled experiment requires exposure of various organisms up to high doses. To meet the gap, Nowack et al. proposed “the SUN approach”: NEPs were micronized to generate fragmented products (FP) in kg quantities for characterization of properties and effects.¹³ Our hypothesis for this study, based on limited reports on mammalian studies, is that FP will have lower environmental impacts compared to pristine ENMs due to the lower surface availability of ENM contained in FPs.

Here, we deliver an exploration of ecological effects of multiple NEP-FPs by multiple ecotoxicity assays, supported by an extensive physical–chemical characterization of the properties of the FPs generated by the SUN approach (Figure 1). Specifically, we compare different ENM in the same matrix and, in addition, explore one ENM in different matrices. We selected a balanced choice of NEPs: this includes highly studied nanomaterials, of which we chose a family of NEPs with multiple walled carbon nanotubes (CNTs) in polyolefins for conductive functionality, in cement for electromagnetic shielding functionality, and in epoxy for lightweight functionality in automotive, construction, and airplane applications, respectively.¹⁴ Additionally, we selected a family of NEP made from less-well-studied ENM from commercially well-established particulate materials, which are now identified as nanomaterials in regulatory terms, specifically transparent halogen-organic and inorganic pigments for automotive parts and coatings.² These constitute the large volume reports in the French nanomaterial registry with above 100 ton/year nanoform production or import in France,

far above CNT.¹⁵ Due to the history of widespread use of nanoforms of these materials in coating, ink, and plastic components of consumer products, a historical and ongoing dispersive emission of NEP fragments into the environment has to be anticipated. We previously verified that the ENMs are present in and on the FPs and that even after extensive (365 MJ/m²) UV radiation, less than 6 ppb of the ENM content migrates or leaches from the weathered FPs (WFPs),¹⁶ such that testing of environmental effects can be approximated by testing FP only. This reasoning is specific to environmentally persistent matrices such as polyolefins or cements, as tested here. Our study is the first to enable their environmental risk assessment with full consideration of the nanostructures induced by the ENM content.

■ MATERIALS AND METHODS

ENM, Synthesis Phase, and NEP, Formulation Phase.

The test panel consisted of three ENM and four matrices. The same nanomaterials have been used previously for extensive human toxicity testing.^{17,18} “CNT” designates multiwall CNT, CAS 308068-56-6, and is the identical grade as the batch distributed as NM400 in the OECD sponsorship program. “OrgPig” designates diketo-pyrrolo-pyrrole, CAS 84632-65-5. “Fe₂O₃” designates hematite, CAS 1309-37-1 (Table SI_1). All ENM were formulated into polyolefins (high-density polyethylene, HDPE, and polypropylene, PP). Additionally to PP, the CNT was integrated in three complementary matrices: polyoxymethylene (“POM”) nanocomposite identical to the FP used in a human tox study,¹⁹ cement (“cement”) nanocomposite identical to the FP used in a human tox study,¹⁹ and epoxy (“epoxy”) nanocomposites identical to those applied in the NanoRelease interlab testing (Table SI_2).²⁰ Comparative testing of environmental weathering releases was performed on the identical nanocomposites, finding release rates that increase across 5 orders of magnitude in the order of polyolefin–POM–epoxy–cement.²¹

NEP Fragmentation, Use Phase. We implemented the SUN approach (Figure 1) and performed cryo-milling for all NEPs as listed in Table SI_2. In short, the OrgPig_PP, Fe₂O₃_PE, CNT_epoxy, and CNT_PP nanocomposite materials and the PP, PE, and epoxy nanofree controls were frozen to cryogenic temperatures (at –193 °C in liquid N₂) to maximize brittleness.¹³ Additionally, to remain comparable to earlier human tox investigations on sanding dusts, limited tests were performed on CNT_POM and CNT_cement fragments and their POM and cement control fragments. These were generated by sanding (1.8 m/s, grit 80, 10 N) of the same NEP batch that was previously investigated by rat in vivo studies.¹⁹ See the Supporting Information for fragmentation details.

FP Size Analysis. Size distributions have been previously reported¹³ and are included by the median diameters here. In short, FP were dispersed in a concentration of 1 g/L by sonication in water containing 0.5 g/L SDS (sodiumdodecylsulfate), and were characterized by laser diffraction (Malvern Mastersizer 3000).

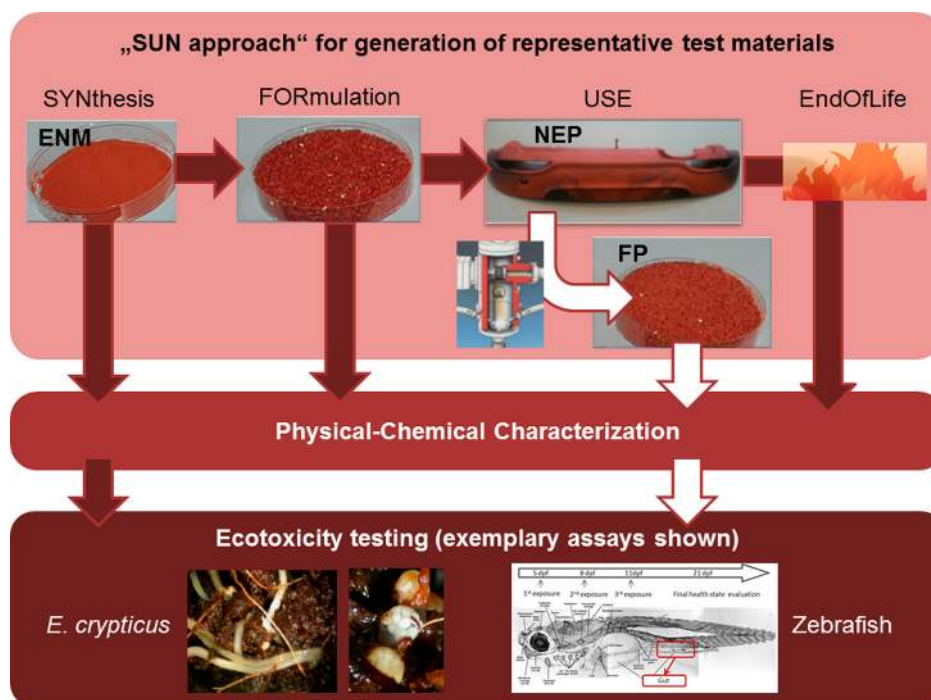


Figure 1. Assessment of environmental impacts from nanoenabled products. Representative test materials across all lifecycle phases are needed: the pristine ENM powder (here, an organic pigment) represents spills during nanomaterial synthesis (SYN), and the pigment-in-polymer master-batch granules represent spills during formulation (FOR). However, the nanoenabled product (NEP), a 1.4 m wide car bumper in one of our case studies, releases fragments only at very slow rates.¹² Specifically to the SUN approach, highlighted by white arrows, mechanical micronisation generates fragmented products (FP) to represent the real-world NEP releases with greatly increased surface and surface-accessible ENM.¹³ Photographs illustrate test materials in 10 cm Petri dishes (no ashes remain after incineration in the specific case). Materials representing all lifecycle phases were compared regarding their physical and chemical properties. The most relevant materials were compared regarding their ecotoxicity by multiple assays, of which the lower panels show Enchytraeids (soil), *Enchytraeus crypticus*, in culture soil and a detail of the cocoons with eggs inside and the zebrafish (aquatic), *Danio rerio*, development assay using water-accommodated fractions. We assessed six NEPs and their ENM-free control matrices in a systematic variation of ENMs and of matrices (see Figure 3).

FP Composition Analysis. The content of ENM in several FP was not known previously and was investigated here by inductively coupled plasma mass spectrometry (ICP-MS) for the inorganic ENM and by combustion for the organic pigment. In the case of CNT, the detection was based on the content of Al and Co in the used CNT that remains from their production process. The Al and Co content is known from earlier release investigations on the same batch of CNT_epoxy.²⁰

FP Surface Chemistry Analysis (X-ray Photoelectron Spectroscopy Plus Hydrophobicity). Surface composition was investigated by XPS to determine element concentrations and content of ENM at the fragments' surface. Phi XPS 5500 with 300 W monochromatic Al-K α radiation pass energy for surveys was 117 eV. The XPS penetration depth of 10 nm is around 3 orders of magnitude smaller than the FP diameters. Identical analysis was performed on pristine ENM. To evaluate the hydrophobicity, contact angle measurements were performed by placing a sessile drop of water onto a round pressed plate of ENM or FP, respectively, with a diameter of 3 cm. Triplicates had standard deviations between 2° and 6°.

FP "Biologically Accessible" Fraction of ENM. Biologically accessible ENM are defined as those that are in contact to the surrounding liquids, and are considered as the fraction that can potentially elicit an ENM-specific effect. FP were dispersed in 1% HCl and shaken for up to 22 h. At each sampling, the suspension was left to settle for 10 min, and then an aliquot sample was taken for ICP-MS to determine Al, Co, and Fe concentrations. The HCl concentration chosen is enough to keep traces of these elements

in a truly dissolved state, while it is not expected to significantly corrode the organic matrix. The method was adapted from Schlagenhauf et al.²²

FP "Dispersibility" in Liquid Media. FP were dispersed by testing both bath sonication (30 min, power of 35W) and probe sonication (15 min, power of 100W) into different media, specifically distilled water (DW) plus sodium dodecyl sulfate (SDS) at 20 mM, DW plus Suwannee River Humic acid (SRHA) at 0.2% w/w, and artificial freshwater (AFW, adhered to OECD 203 protocol)²³ plus SRHA at 0.2% w/w. As expected from polyolefin density, flotation of FPs on the water surface was observed. The results were confirmed within the concentrations range from 10 mg/L to 10 g/L by means of dynamic light scattering (DLS, multiangle Nicomp ZLS Z3000 Particle Sizing System), centrifugal separation analysis (CSA, LUMiSizer 651, L.U.M. GmbH), and number-based transient resistive pulse sensing (TRPS, Izon qNano).

Ecotoxicological Testing of Fragmented Material. Testing aimed to cover from aquatic to terrestrial exposure, using a suite of standard organisms and associated endpoints as these are among the current mandatory framework. As shown in Figure 1, each phase of the lifecycle may result in environmental emission by spills during SYN and FOR or by slow micronization and degradation during use or, finally, by landfiling of remaining solids after incineration (polymers) or after destruction (cements), impacting sewage treatment plants, soils, and other compartments.

Sewage Sludge Treatment Plant Function. Effects on the biological function of a sewage treatment plant (STP) were investigated based on the OECD Test Guideline 303A (OECD, 2001).

A lab-scale STP (behrotest Laborkläranlage KLD 4N, Germany) with a denitrification and nitrification reactor and a secondary clarifier was used. The pristine Fe_2O_3 and the fragmented Fe_2O_3 _PE were added continuously over 10 days with the synthetic sewage into the denitrification reactor of the model STP. Effects on the biological function of the STP were assessed by measurements of the elimination rate of dissolved organic carbon and the determination of nitrate, nitrite and ammonia in the effluent of the sewage treatment plant, representing the denitrification and nitrification processes. Treatments included from 0.04 mg/L (environmentally relevant) to 1.0 mg/L (worst case scenario).

Microbial Function: Short and Long-Term Effects on the Soil Microflora. The nitrite content was determined using the short-term potential ammonium oxidation test as recommended by ISO guideline 15685 (2012). The effect on ammonia oxidizing bacteria was determined 24 h and 28 days after application of the nanomaterials (10 and 1000 mg/kg dry matter soil) into reference soil.

Long-Term Effects via Sewage Sludge Spread into Agricultural Soil. After 10 days continuous addition of the nanomaterial into the STP, the sludge was dewatered and added to the reference soil in accordance with the German sewage sludge ordinance, which states that 5 tons per hectare over 3 years can be spread on agricultural areas. A total of 1.67 g of dry matter sludge was introduced into the soil under the assumption of a soil depth of 20 cm and soil density of 1.5 g/m³, corresponding to test concentrations of 0.4 and 10 mg/kg dry matter soil. The soil was incubated at 20 °C in an incubation chamber in the dark. The long-term effect of the nanomaterials added via sewage sludge on the ammonia oxidizing bacteria was investigated after 30, 60, 100, and 140 days of incubation.

Enchytraeid Reproduction Test. Cultures of test species *E. crypticus* (Oligochaeta: Enchytraeidae, Figure 1) were kept in agar plates for several years.²⁴ The standard LUFA 2.2 natural soil (Speyer, Germany) was used. Spiking followed the recommendations for nanomaterials^{25,26} The standard guideline (ISO 2004; OECD 2004) was followed, but instead of using adults, 10 synchronized age (17–18 days) organisms were used. Exposure concentrations ranged from 0 to 3200 mg/kg soil dry weight for both the ENM and the FP, i.e., for the FP exposure there was a corresponding lower percentage of ENM. The tests were run at 20 °C and a 16:8 light/dark h photoperiod during a period of 28 days. Endpoints assessed included survival (number of adults) and reproduction (number of juveniles).

Hatching, Survival, and Growth Test on Zebrafish Embryos and Larvae. Zebrafish embryos and larvae were used to assess the hazard potential in a model organism frequently used in nanomaterial safety studies (Figure 1). Motivated by FP hydrophobicity and lack of dispersibility, sample preparation for aquatic compartment testing (see details in the Supporting Information) targeted the water-accommodated fraction as recommended by an OECD workshop.²⁷ Healthy embryos at the same developmental stage (2 h post-fertilization, hpf) were selected and placed in 96-well plates with one embryo per well.^{28,29} A total of 100 μL of CNT or FP of CNT–cement and CNT–POM was added to the wells at 4 hpf. To achieve robust statistical calculation, 5 replicate trials were carried out, each using 12 embryos. Observations of adverse biological outcomes, including hatching interference, phenotypic abnormalities, and mortality (necrosis of the embryos), were carried out every 24 h for 5 consecutive days.

Using our previously developed pulse exposure procedure,³⁰ we further investigated the hazard potential of the CNT and FP

from CNT nanocomposites in zebrafish larvae. As shown in Figure SI_5, the pulse exposure was conducted using groups of 30 growth-synchronized larvae at 5, 8, and 11 days post-fertilization (dpf). The exposure was performed in Petri dishes for 6 h each time by immersing the larvae in 3 mL of the suspension of CNT or FP. The larvae were maintained in standard aquarium tanks for further observation of development and survival until 21 dpf. The overall health status of the larvae was assessed at 14 dpf based on gross morphology, body length and weight, and number of calcified vertebrae. To assess morphology, larvae were anesthetized in 0.02% tricaine and embedded in low-melt agarose gel. This allowed positioning to obtain lateral views to assess morphology, body length, and fin structure.

Cytotoxicity on Fish Cell Lines. A pair of fish-derived cell lines were used: RTL-W1³¹ and CLC.^{32,33} For details, see the Supporting Information. Cells were exposed for 24 h to appropriate concentrations of the original NM or of the FP (0.78 to 100 $\mu\text{g}/\text{mL}$) using 96 well plates. A pair of independent experiments were carried out, with treatments applied in triplicate in each experiment. Fresh suspensions were prepared for each experiment in Milli-Q water at 10 mg/mL by sonication for 20 min in an ice–water bath using a probe sonicator (Vibra cell VCX130, Sonics & Materials Inc., Newtown, CT) (2 mm microtip, 80% of amplitude continuous mode). A total of 75 μL was then mixed with 25 μL of bovine serum albumin (BSA, 80 mg/L) solution, added to 7.4 mL of culture medium, and sonicated for 10 min in a bath sonicator (S 40 H Elmasonic, Elma, Germany). Cells were exposed to 1/2 serial dilutions of this suspension in culture medium. Cytotoxicity was measured by three different assays.^{34,35}

RESULTS AND DISCUSSION

Enabled by the SUN approach (Figure 1), we followed nanomaterials along their lifecycle, both by physical–chemical and by ecological methods. The pristine ENM, representing the synthesized (SYN) phase, and the fragmented product, representing releases during the use phase (USE), were characterized in terms of size, composition, and surface properties (Figure 2 and Table SI_3). Additionally, selected properties were available from our previous publications or from gap-filling original data for the formulation (FOR) and end of life (EOL) phases. Figure 3 thus constitutes a “lifelog” of nanomaterials from cradle to grave.

Our specific understanding of lifecycle phases differentiates:

- SYN: synthesis of the pristine ENM, typically as powder. Industrial process by chemical operations. Risk assessment prioritizes occupational human aerosol exposure and environmental emissions by spills and waste streams.
- FOR: formulation of the ENM as an additive in a product matrix. Industrial manufacturing process that produces a nanoenabled product (NEP). Our case studies used ENM masterbatch (for thermoplastic polymers PP, PE, and POM), or ENM suspensions in liquid precursors (epoxy polymer and cement).
- USE: consumer use of the NEP. Risk assessment needs to consider various product-specific scenarios with durations between days and decades. For our specific case studies, environmental emissions of FP by weathering and wear and tear during outdoor use take priority.
- EOL: end of life of the NEP by recycling or disposal by incineration or landfill. For our specific case studies, Table SI_3 reports the results measured for incineration of epoxy³⁶ and PP^{37,38} or landfill of cement FP.

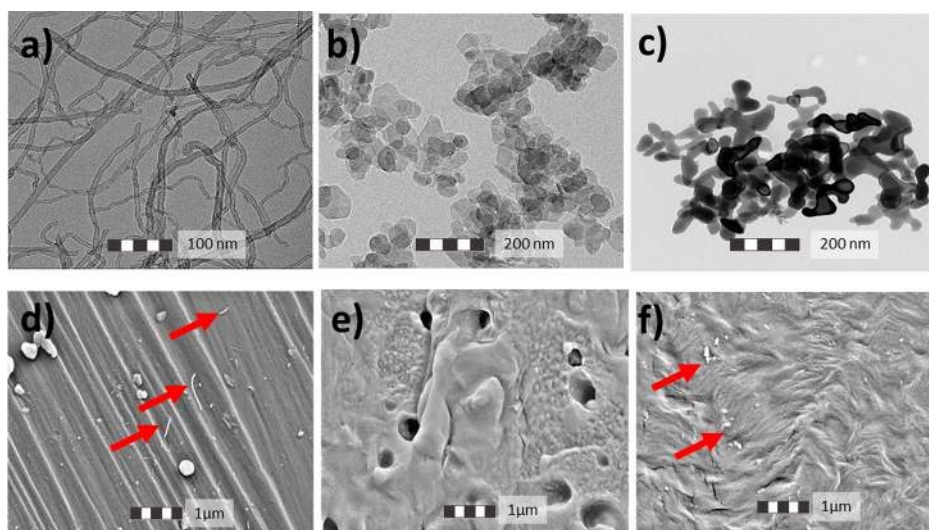


Figure 2. SEM scans to characterize surface structures of (a–c) ENM (representative for lifecycle SYN phase) and (d–f) fragments of NEP containing the same ENM (FP, representative for lifecycle USE phase). (a) CNT, (b) halogen-organic diketopyrrolopyrrole pigment red 254 (OrgPig), (c) Fe_2O_3 pigment red 101, (d) FP of nanocomposite CNT_epoxy, (e) FP of nanocomposite OrgPig_PP, and (f) FP of nanocomposite Fe_2O_3 _PE. Red arrows highlight protrusions of ENM on FP surfaces. See Figure SI_1 for pure matrix control fragments and whole-particle scans.

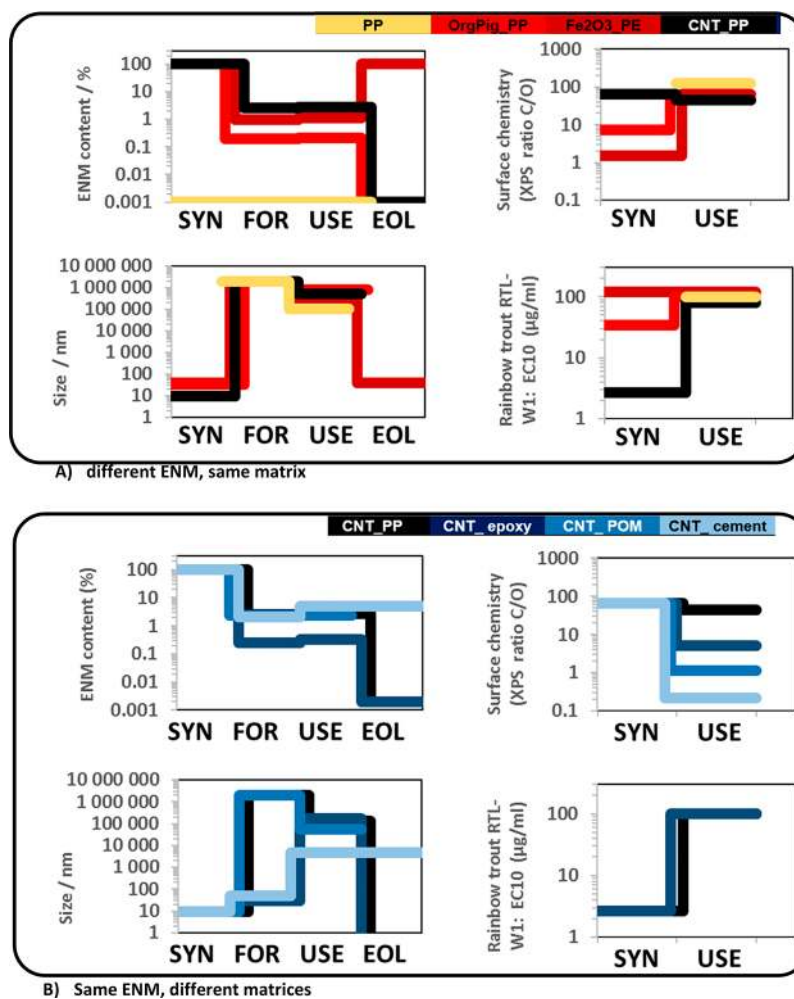


Figure 3. Tracking nanoenabled products along the lifecycle stages SYNthesis, FORMulation, USE, and end of life: (A) different ENM, same matrix and (B) same ENM, different matrices. Panels summarize the key descriptors of size (median diameter), composition (ENM content), surface chemistry (C-to-O ratio), and ecotoxicity (represented by our most sensitive assay, rainbow trout RTL-W1). Ecotoxicity EC10 values are lower limits for the USE phase. The color-coding of NEPs is indicated above the figure. See the beginning of the Results and Discussion section for the scenario assumptions on the SYN, FOR, USE, and EOL phases.

Previously, we reported the FP size as a basic descriptor.¹³ Here, we go further to characterize the composition and surface chemistry by several descriptors that are most relevant for nanoscale- or microparticles. The actual ENM content in FP (USE phase) was found to be minimally above the ENM content of the FOR phase, resulting in a small kink in the “nanomaterial lifelog” between the FOR and USE phases (Figure 3, panel “composition”). The increase in ENM content correlates roughly with the brittleness of the matrix because it is, at least with PP and PE, higher with epoxy and cement. Transmission electron microscopy (TEM) scans of iron oxide pigments extracted from Fe₂O₃_PE fragments showed no significant change of nanomaterial structure due to the fragmentation process (ultramicrotomy data not shown). Because the changes of composition are minimal between FOR phase and USE phase (Figure 3 and Table SI_3), whereas only the USE phase potentially releases fragmented product by diffuse emissions into the environment, we focused testing on the SYN and USE phases. Sizes after sieving were above the inhalable range for all cryo-milled FP (Figure 3, panel “size”), in accord between laser diffraction, suspension-based analytics and microscopy.¹³ The amounts of the sieved fragments were below 0.5% of cryomilling output and were provided for ecotoxicological testing. Additionally, FPs produced by sanding CNT_POM_FP were consistent in size with the other FP generated by cryo-milling, as the CNT_POM_FP had <1% passed through a 2.7 μm filter, and <60 ppm were below 0.1 μm (both with and without CNT); 3% of the CNT_cement_FP passed through a 2.7 μm filter, and 100 ppm were below 0.1 μm.¹⁹ High-resolution images reveal protrusions of the inorganic Fe₂O₃ pigment and CNTs at the surface of corresponding fragments (red arrows in Figure 2), whereas the lower concentration and lower electron density of OrgPig caution against an interpretation of absence of protrusions from SEM results.

“Protrusions”^{22,39} of ENM on the surface of fragments were investigated by multiple approaches: surface chemistry (XPS, elements, and C(1s) line shift identification), hydrophobicity (sessile water drop contact angle), and morphology scanning electron microscopy (SEM). As hypothesized in the introduction, the surface of all investigated FP materials is mainly composed of carbon (Table SI_3 and Figure 3, panel “surface chemistry”). In case of the epoxy-based materials, further elements such as carbon and nitrogen are present in higher contents as well. The XPS quantification of different species by C(1s) line shift (Figure SI_2) analysis finds a surface content of CNT in CNT_PP_FP of 4.3%, which is slightly increased above the bulk content determined by ICP-MS of 2.7%. Also the Al and Co acid leaching analysis showed that the CNT are accessible to the liquid phase on the surface of the CNT_PP fragments, as these released Co and Al (Figure SI_3). The biologically accessible concentration of Al was deduced to be 27.0 μg/m² on FP with CNT and 7.6 μg/m² without; the respective values for Co were 2.3 and 0.1 μg/m² (Table SI_4 and calculation therein). Correcting for the control background, and using the diameter, density, and metal content in this specific CNT grade, we deduced from the acid leaching that 6.2% of the surface area provide contact to CNT. Considering the approximations made, this value is in excellent accord with the XPS result and predicts that protrusions of ENM modulate the surface chemistry of FP but do not dominate it. For CNT in epoxy and for Fe₂O₃ in PP, however, leaching results are convoluted by contaminations of the matrix with the target analytes (Al, Fe) (results in the Supporting Information). Further work will aim at determining whether these metals are embedded in the NEP or if the NEP

fragmentation process contaminates the FP. The same methods of XPS line shift, tracer ion release and TEM analysis, found significant protrusions on brittle CNT_epoxy²² or CNT_cement³⁹ but low prevalence in tough materials such as CNT_POM or CNT_PP.^{39,40} This is in accord with our results.

For organic pigment, XPS line shape analysis identifies an enrichment at the FP surface with up to 9% on the FP surface compared to 0.21% within the FP bulk (Figure SI_2) but may be less reliable because only CNTs emit C(1s) photoelectrons at a distinct energy shift, whereas the organic pigment signal overlaps with the PP matrix signal. The water contact angle was considered as simple measure of surface-mediated (extrinsic) interactions. The contact angle results highlight that the FP surface hydrophobicity is clearly dominated by the matrix, not by the ENM (Figure 3 panel “surface chemistry” and Figure SI_7).

Surface chemistry controls nanobiointeractions but also impacts fate and transport. In biologically irrelevant media such as a 1:1 acetone:water mixture, the FP can be solubilized and dispersed, but in environmentally relevant media such as artificial fresh water with or without natural organic matter, the FP remain agglomerated and tend to float (especially the polyolefins PE and PP). In accordance to the results from laser diffraction reported earlier,¹³ no significant fraction below 1 μm diameter was detected by measurements with the nanospecific methods of DLS and CSA, using either SDS or SRHA as dispersants. By the nanospecific counting method of TRPS, all FP showed the presence of fragments in a size range between 200 and 800 nm, but the number-based concentrations ranged between 10⁶ and 10⁷ no./mL for 10 g/L FP suspensions (Table SI_5). This converts to a low parts per million level mass content of fragments with diameters below 1 μm. In a very-condensed presentation of size, surface chemistry, and composition, Figure 3 summarizes the dramatic changes of physical–chemical properties along the NEP lifecycle.

■ ECOTOXICITY EFFECT CHARACTERIZATION

No hatching or survival rate of zebrafish embryos were affected by CNT or the FP (Figure SI_5), likely due to low heavy-metal content from the CNT and little to no penetration through the chorion of the embryos. With the pore size of the chorion being at the range of 200–500 nm, it was anticipated that there was little to none penetration of CNT and FP into the chorionic space. As shown in Figure 4, both CNT and CNT composites showed little to no toxicity as reflected by the survival and growth of zebrafish larvae subject to aqueous exposure. Even though in the zebrafish assay CNT were protruding and entirely biologically accessible after shaking in solution or sonication from CNT–cement_FP (Figure SI_4), whereas there was no protrusion from CNT–POM_FP, the composites showed no adverse effects on zebrafish embryo hatching or on the survival and growth of zebrafish larvae. These results show that CNT nanocomposites do not appear to have negative impact on zebrafish. Zebrafish embryo hatching was previously demonstrated to be affected by heavy metal ions, such as Zn²⁺, Cu²⁺, Ni²⁺, and Cr³⁺.²⁸ The lack of hatching interference observed here suggests that the heavy metal leaching, observed only in HCl to reach parts per billion levels during 22 h (Figure SI_3), remained low during the test but may contribute to long-term effects in the environment. One may differentiate that only free ENM are biologically available in the sense that they can be taken up, whereas ENM protrusion on a larger fragment are only accessible in the sense that they interact with, e.g., the chorion or cell membrane.

Results of the toxicity of the original material and of the FP (SYN and USE phases, respectively) on RTL-W1 cells, repre-

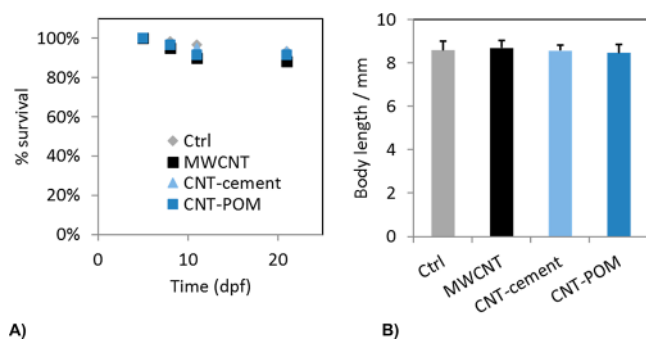


Figure 4. Aquatic compartment screening on zebrafish larvae. Both (A) survival (standard deviation of $N = 30$ replicates were determined for each time point and were below 5% for all) and (B) body length at day 14 showed no statistically significant differences between the control and exposure of CNT and FP. Pulse exposure was performed on 5, 8, and 11 days post-fertilization (dpf) (see scheme in Figure 1). See Figure SI_5 for zebrafish embryo development and growth results.

sented as the most sensitive assay, are summarized by Figures 3 and SI_6. In both fish cell lines, RTL-W1 and CLC, the original NM (SYN phase) caused decreased cell viability. The lowest EC_{50} was detected in RTL-W1 cells by means of the 5-carboxy-fluorescein diacetate acetoxyethyl ester (CFDA-AM) assay, $23.56 \pm 5.0 \mu\text{g/mL}$. The toxicity in the CLC cells was below EC_{50} ; hence, this was not calculated. The exposure of cells to the FP (USE phase) did not cause any toxicity, even at the maximal concentration used, $100 \mu\text{g FP/mL}$. However, $100 \mu\text{g FP/mL}$ contains nanomaterials at $<5 \mu\text{g/mL}$. In addition to this low concentration of NM, the low density of FPs causes their flotation, and hence, the contact with the cells was minimal. Other alternatives, as cells in suspension instead of attached to the bottom of the plates or an inverted culture should be tested in future to enhance the sensitivity of the assay, as demonstrated for PP-based incineration-FPs.^{41,42}

On ammonia oxidizing bacteria, the reference products and the pristine nanomaterials Fe_2O_3 Red 101, Organic Pigment Red 254, and CNT showed no effects at test initiation and after 28 days. A comparable result was found for the fragmented products Fe_2O_3 _PE, OrgPig_PP, and CNT_epoxy, although for Fe_2O_3 _PE and CNT_epoxy at 1000 mg/kg dry matter soil inhibitory effects of 23% and 38%, respectively, were determined at test start. However, this effect could not be confirmed after 28 days of incubation. The results are presented in Table SI_4. Thus, after 28 days, EC_{50} values were above 1000 mg/kg dry matter soil for all products tested. No impact occurred on the biological function/microbial activity of the sewage sludge, neither on the elimination of dissolved organic carbon nor on the denitrification and nitrification processes. There were no effects due to the pristine and fragmented products observed on the activity of the ammonia oxidizing bacteria over 140 days after application of the nanomaterials via sewage sludge into soil.

Results for *E. crypticus* showed no effects on survival for any of the FP (Figures 3, SI_7, and SI_8). Effects in terms of reproduction showed increased sensitivity, with the pure NM (SYN phase) having different EC_{10} ; specifically, OrgPig had a measurable effect ($EC_{10} = 2009 \text{ mg/kg}$) but not Fe_2O_3 or CNT. All FP, both NM-containing FP and the pure polymer FP (pure PE, pure epoxy, and pure PP), caused no effect in the tested range ($0\text{--}3200 \text{ mg/kg}$). Such results are not unexpected given the low degradability of the tested matrix or the low fraction of NM embedded in the matrix. The added characterization of the NEP further confirms the hypothesis. Of note, for OrgPig_FP, a 10%

reduction in reproduction occurs for 800 mg/kg although no effects occurred at higher concentrations. A nonmonotone dose response has been reported before for Ag²⁶ and Ni.⁴³ This could be related to the potentially reduced agglomeration at lower concentrations hence higher exposure and effects. However, we do not have evidence to support this hypothesis for the FP with or without embedded ENMs.

Figure 3 and Table 1 summarize the results of our explorations. At the ENM concentrations tested, the NEP matrix properties dominated the intrinsic and extrinsic FP properties, including their ecotoxicity in a wide range of assays covering sludge, soil, and fish. A pair of orthogonal comparisons help identify the mechanisms:

- (1) The surface chemistry, hydrophobicity and the size of fragments assimilate in the use phase of different ENM in the same matrix (Figures 3a and SI_7).
- (2) Conversely, for one type of ENM in NEPs with different matrices, the surface chemistry and size of the use-phase fragments diversifies (Figure 3b).

Both categories of lifecycle-induced ENM transformation, assimilation of properties and diversification of properties by product formulation and fragmentation, have been predicted earlier by Mitrano et al.¹⁰ Here, we studied specific examples with polymeric and cementitious matrices with organic, carbonaceous, and inorganic ENM and explore their implications for environmental hazards. In both transformation categories, we find that the physical–chemical properties of the bulk matrix predominantly determine the physical–chemical properties of the fragments released during USE, with little modulation by the ENM that was embedded in the NEP. With the specific ENM and matrices, the ecotoxicity of fragments released during the lifecycle of NEPs is not affected by the ENM.

However, the validity of each individual ecotoxicity assay (that were not developed for FP testing) is challenged by one or other FP property. For some materials (low density of polyolefins) floatation limits the delivered dose; this is, however, no issue for FP testing of epoxy, POM, and cement, which are denser than water. Further, the size range of the tested fragments is larger than generally adequate for the tests and species. To reduce this uncertainty, we sieved away 99.5% of the larger particles so that exposure was targeted to smallest sizes. Yet, for organisms such as *E. crypticus*, the FP sample contains fragments that can be larger than the organisms themselves. A detailed discussion can be found in a recent opinion paper.⁴⁴ Enchytraeids and other oligochaetes are exposed via soil ingestion and skin adsorption; hence, in this case, risk is reduced or absent via exposure. Also, the absence of adverse effects on the microbial soil compartment are at least partially due to the reduction of exposure because the thermoplastic matrices have low degradation and diffusion.^{9,45} No effects on soil microflora were found for relatively long periods up to 140 days, but a high bacterial resilience may also contribute to this absence of effects. Follow-up options include long-term aging of FPs before testing or much longer term biota exposure. Additional species can be added, e.g., filter feeding marine organisms may be susceptible to both direct effects of microplastic particles⁴⁶ and to vector effects of adsorbed toxicants.⁴⁷ One may speculate that toxicant affinity is modulated by the surface chemistry, even if we found surface chemistry to be dominated by the matrix, not by the ENM.

There is no directly comparable study on nanocomposites. One paper reported an unconventional ecotoxicity assay by exposing fruit flies to an environmentally aged CNT composite, finding

Table 1. Effects of Use-Phase Fragmented Product Tested in Various Ecotoxicity Assays^a

| | PP | OrgPig_PP | Fe ₂ O ₃ _PE | CNT_PP | CNT_epoxy | CNT_POM | CNT_cement |
|---------------------------------|-------------|-------------|------------------------------------|-------------|-------------|--------------|--------------|
| RTL-W1 EC10 | >100 μg/mL | >100 μg/mL | >100 μg/mL | >100 μg/mL | >100 μg/mL | NT | NT |
| CLC EC10 | >100 μg/mL | >100 μg/mL | >100 μg/mL | >100 μg/mL | >100 μg/mL | NT | NT |
| soil microflora EC10 | >1000 mg/kg | >1000 mg/kg | >1000 mg/kg | NT | >1000 mg/kg | NT | NT |
| STP biology EC10 | NT | NT | >6000 mg/kg | NT | NT | NT | NT |
| <i>E. crypticus</i> EC10 repro. | >3200 mg/kg | >3200 mg/kg | >3200 mg/kg | >3200 mg/kg | >3200 mg/kg | NT | NT |
| ZF embryo NOAEL | NT | NT | NT | NT | NT | >5 mg/embryo | >5 mg/embryo |
| ZF larvae NOAEL | NT | NT | NT | NT | NT | >50 mg/mL | >50 mg/mL |

^aNo FP elicits a significant effect. NT: not tested. RTL-W1, fibroblast from biliary ducts of rainbow trout. CLC, macrophage cell line from carp. *Enchytraeus crypticus* survival is not affected, and the results reported are EC10 of reproduction. The soil microflora short-term potential ammonium oxidation test based on ISO Guideline 15685. For STP biology the biological function of a sewage treatment plant (STP) was based on OECD Guideline 303A. For ZF embryos, zebrafish embryos exposed to the water-accommodated fraction of the FP mass indicated, assessing hatching percentage and survival rate vs control embryos. For ZF larvae, zebrafish larvae exposed repeatedly to the water-accommodated fraction of the FP concentration indicated, assessing body length and survival rate vs control larvae.

no specific effects.⁴⁸ A total of seven papers assessed the toxicity for humans by sanding fragments released from NEPs and focused on inhalation exposure^{19,22,49–53} and oral exposure.⁵⁴ For paints and plastics NEPs with silica, titania, and CNT additives, the studies report no additional toxicity by the ENM in the primary target organ,^{19,22,49–54} only one study found secondary effects in the liver.⁵⁵ Models for environmental risk assessment currently assume the fate and effects of NEP to be determined by ENM properties.⁶ This assumption needs to be revisited in light of the present finding of NEP environmental effects determined by matrix properties and of their significant differences in key physical–chemical properties such as composition, size, and surface chemistry.¹¹ We designed the studies to explore the possible modulation of ecotoxicity by nanomaterial additives in plastics, polymer, and cement. We found no such modulation despite a systematic variation of different nanomaterials (Figure 3A) and different matrices (Figure 3B) and test organisms representing different environmental compartments (Table 1). In a separate paper, the predicted environmental concentrations (PEC) based on material-flow exposure models for nanomaterials and predicted no-effect concentrations (PNEC) were estimated with species sensitivity distribution models. PEC-to-PNEC risk ratios were obtained for the case studies, species, and environmental compartments described above and indicate no risks based on the given data.⁵⁵

With regard to our primary motivation by nanomaterial risk assessment, the present results lend support to grouping of ecotoxicity during the use phase; the group would be defined by the matrix material, potentially limited to a certain maximum ENM content that is relevant for ENM application as functional additive (typically below 5%). The ecotoxicity of fragments emitted during the use phase would be read across from the pure matrix material. The grouping by matrix would probably fail for easily hydrolysible matrices,⁸ which would release free ENM and were not tested here, and for NEPs using dissolving ENM such as Ag and CdTe, which were tested and reviewed elsewhere.^{9,56–58} Furthermore, secondary fragmentation and release of free ENM may occur during transport to the final sink in soils or sediments over time scales longer than the standard test duration for organisms. However, secondary ENM release by weathering and migration was independently tested on the identical NEP, and strong containment by the polyolefin matrix was found.¹⁶ Another experimental study on tire wear found up to 0.045% releases of free ENM for secondary UV/hydrolysis degradation, as this only affects a sub-micrometer-thin surface layer of many-micrometer-diameter FP particles.⁵⁹ Furthermore, any secondary fragmentation by UV degradation is again mostly

determined by the matrix, with benchmarks of labile (epoxy), intermediate (polyamide) and resilient (PE, PP, and cement) matrices.²¹ Thus, grouping by matrix can be applied to a wide range of matrices and ENM that is delimited by the intended persistence during use.

As a secondary interpretation, one may identify the FP material as microplastics. The size range and composition match the definition of, e.g., the Danish Environmental Protection Agency.⁶⁰ Plastics, including commodity plastics with widespread use, are routinely colored with pigments such as Fe₂O₃, whereas the Organic Pigment Red 254 is rather a high-performance pigment class, and CNTs are currently a lower-volume material.¹⁵ Our results on PP, POM, epoxy and PE, with and without ENM, can be interpreted as one of the first studies on the effects of microplastics on organisms in soils, fish, and on the sewage treatment plant biological activity. We found no significant effects up to the highest concentration tested. Of note, considerations of physical–chemical similarity as proposed by Hüffer et al.¹¹ would position our mechanically shredded plastics with hydrophobic, irregular surfaces and low aquatic dispersibility as more similar to real-world secondary microplastics of polyolefin (packaging), polyamide (fishery nets),⁶¹ or rubber (tire wear)⁶⁰ than charge-stabilized polystyrene beads that are simply more convenient in (eco)toxicity assays.⁶² The SUN approach thus contributes to the environmental hazard screening of both nano- and microstructures.

■ ASSOCIATED CONTENT

📄 Supporting Information

The Supporting Information is available free of charge on the ACS Publications website at DOI: 10.1021/acs.est.7b04122.

Tables showing nanomaterials, matrices of nanoenabled products, physical and chemical properties along the synthesis lifecycle, biologically accessible tracers of CNT, number-based suspension characterization, and effects caused by pristine and fragmented materials. Additional data on NEP fragmentation processes, surface chemistry, the preparation of materials for zebrafish testing, and details on methods and results with cell lines. Figures showing additional SEM scans of shape and surface structure of FPs, the results of the line-shape analysis, dissolved aluminum and cobalt concentration, the preparation of water-accommodated fractions, aquatic compartment screening on zebrafish embryos, cytotoxicity of multiple-wall carbon nanotubes and of fragmented products, and survival and reproduction results. (PDF)

AUTHOR INFORMATION

ORCID

Mónica J.B. Amorim: 0000-0001-8137-3295

Sijie Lin: 0000-0002-6970-8221

Tian Xia: 0000-0003-0123-1305

André Nel: 0000-0002-5232-4686

Wendel Wohlleben: 0000-0003-2094-3260

Notes

The authors declare the following competing financial interest(s): KV, NN, WW are employees of a company producing and marketing nanomaterials.

ACKNOWLEDGMENTS

This work was supported by the project on Sustainable Nanotechnologies (SUN) that receives funding from the European Union Seventh Framework Programme (FP7/2007–2013) under grant agreement n° 604305. Thanks are also due for the support to CESAM (UID/AMB/50017 - POCI-01-0145-FEDER-007638), to FCT/MCTES through national (PIDDAC), and the co-funding by FEDER, within the PT2020 Partnership Agreement and Compete 2020. Work by SL, TX and AN was supported by the National Science Foundation and the Environmental Protection Agency under Award No. DBI-1266377.

ABBREVIATIONS

| | |
|---------|---|
| AFW | artificial freshwater |
| BSA | bovine serum albumin |
| CFDA-MS | 5-carboxyfluorescein diacetate acetoxyethyl ester |
| CNTs | carbon nanotubes |
| CSA | centrifugal separation analysis |
| DLS | dynamic light scattering |
| dpf | days post-fertilization |
| DW | distilled water |
| EOL | end of life |
| ENM | pristine engineered nanomaterials |
| ERT | enchytraeid reproduction test |
| FOR | formulation |
| FP | fragmented products |
| HDPE | high-density polyethylene |
| hpf | hour post-fertilization |
| NEPs | nanoenabled products |
| OrgPig | diketo-pyrrolo-pyrrole |
| PE | polyethylene |
| PEC | predicted environmental concentrations |
| PNEC | predicted no effect concentrations |
| POM | polyoxymethylene |
| PP | polypropylene |
| SDS | sodiumdodecylsulfate |
| SEM | scanning electron microscopy |
| SRHA | Suwannee river humic acid |
| STP | sewage treatment plant |
| SYN | synthesis |
| TEM | transmission electron microscopy |
| TRPS | transient resistive pulse sensing |
| WFPS | weathered fragmented products |
| XPS | X-ray photoelectron spectroscopy |

REFERENCES

(1) Stark, W.; Stoessel, P.; Wohlleben, W.; Hafner, A. Industrial applications of nanoparticles. *Chem. Soc. Rev.* **2015**, *44* (16), 5793–5805.

(2) Wohlleben, W.; Punckt, C.; Aghassi-Hagmann, J.; Siebers, F.; Menzel, F.; Esken, D.; Drexel, C.-P.; Zoz, H.; Benz, H. U.; Weier, A.; Hitzler, M.; Schäfer, A. I.; Cola, L. D.; Prasetyanto, E. A. Nanoenabled Products: Categories, Manufacture, and Applications: Protocols and Industrial Innovations. In *Metrology and Standardization for Nanotechnology: Protocols and Industrial Innovations*, Mansfield, E.; Kaiser, D. L.; Fujita, D.; Van de Voorde, M., Eds. John Wiley & Sons: Hoboken, NJ, 2017; pp 411–464.

(3) Harper, S.; Wohlleben, W.; Doa, M.; Nowack, B.; Clancy, S.; Canady, R.; Maynard, A. Measuring nanomaterial release from carbon nanotube composites: review of the state of the science. *J. Phys.: Conf. Ser.* **2015**, *617* (1), 012026.

(4) Nowack, B.; David, R. M.; Fissan, H.; Morris, H.; Shatkin, J. A.; Stintz, M.; Zepp, R.; Brouwer, D. Potential release scenarios for carbon nanotubes used in composites. *Environ. Int.* **2013**, *59*, 1–11.

(5) Sun, T.; Mitrano, D. M.; Bornhöft, N. A.; Scheringer, M.; Hungerbuehler, K.; Nowack, B. Envisioning nano release dynamics in a changing world: using dynamic probabilistic modelling to assess future environmental emissions of engineered nanoparticles. *Environ. Sci. Technol.* **2017**.51285410.1021/acs.est.6b05702

(6) Garner, K. L.; Suh, S.; Keller, A. A. Assessing the Risk of Engineered Nanomaterials in the Environment: Development and Application of the nanoFate Model. *Environ. Sci. Technol.* **2017**, *51* (10), 5541–5551.

(7) Hund-Rinke, K.; Baun, A.; Cupi, D.; Fernandes, T. F.; Handy, R.; Kinross, J. H.; Navas, J. M.; Peijnenburg, W.; Schlich, K.; Shaw, B. J.; et al. Regulatory ecotoxicity testing of nanomaterials—proposed modifications of OECD test guidelines based on laboratory experience with silver and titanium dioxide nanoparticles. *Nanotoxicology* **2016**, *10* (10), 1442–1447.

(8) Duncan, T. V. Release of Engineered Nanomaterials from Polymer Nanocomposites: the Effects of Matrix Degradation. *ACS Appl. Mater. Interfaces* **2015**, *7*, 20–39.

(9) Duncan, T. V.; Pillai, K. Release of Engineered Nanomaterials from Polymer Nanocomposites: Diffusion, Dissolution, and Desorption. *ACS Appl. Mater. Interfaces* **2015**, *7* (1), 2–19.

(10) Mitrano, D. M.; Motellier, S.; Clavaguera, S.; Nowack, B. Review of nanomaterial aging and transformations through the life cycle of nano-enhanced products. *Environ. Int.* **2015**, *77* (0), 132–147.

(11) Hüffer, T.; Praetorius, A.; Wagner, S.; Von Der Kammer, F.; Hofmann, T. Microplastic exposure assessment in aquatic environments: learning from similarities and differences to engineered nanoparticles. *Environ. Sci. Technol.* **2017**.51249910.1021/acs.est.6b04054

(12) Koivisto, A. J.; Jensen, A. C. Ø.; Kling, K. I.; Nørgaard, A.; Brinch, A.; Christensen, F.; Jensen, K. A. Quantitative material releases from products and articles containing manufactured nanomaterials: Towards a release library. *NanoImpact* **2017**.511910.1016/j.impact.2017.02.001

(13) Nowack, B.; Boldrin, A.; Caballero, A.; Hansen, S. F.; Gottschalk, F.; Heggelund, L.; Hennig, M.; Mackevica, A.; Maes, H.; Navratilova, J. Meeting the Needs for Released Nanomaterials Required for Further Testing—The SUN Approach. *Environ. Sci. Technol.* **2016**, *50* (6), 2747–2753.

(14) Zhang, J.; Terrones, M.; Park, C. R.; Mukherjee, R.; Monthieux, M.; Koratkar, N.; Kim, Y. S.; Hurt, R.; Frackowiak, E.; Enoki, T.; Chen, Y.; Chen, Y.; Bianco, A. Carbon science in 2016: Status, challenges and perspectives. *Carbon* **2016**, *98*, 708–732.

(15) Ministère de l'Environnement: Paris, accessible at <https://www.r-nano.fr/>. Éléments issus des déclarations des substances à l'état nanoparticulaire: Exercice 2015. **2015**.

(16) Neubauer, N.; Scifo, L.; Navratilova, J.; Gondikas, A.; Mackevica, A.; Borschneck, D.; Chaurand, P.; Vidal, V.; Rose, J.; von der Kammer, F.; Wohlleben, W. Nanoscale Coloristic Pigments: Upper Limits on Releases from Pigmented Plastic during Environmental Aging, In Food Contact, and by Leaching. *Environ. Sci. Technol.* **2017**, *51* (20), 11669–11680.

(17) Hofmann, T.; Ma-Hock, L.; Strauss, V.; Treumann, S.; Rey Moreno, M.; Neubauer, N.; Wohlleben, W.; Gröters, S.; Wiench, K.; Veith, U.; Teubner, W.; van Ravenzwaay, B.; Landsiedel, R. Comparative short-term inhalation toxicity of five organic diketopyrro-

lopyrrole pigments and two inorganic iron-oxide-based pigments. *Inhalation Toxicol.* **2016**, *28*, 463.

(18) Ma-Hock, L.; Strauss, V.; Treumann, S.; Küttler, K.; Wohlleben, W.; Hofmann, T.; Gröters, S.; Wiench, K.; van Ravenzwaay, B.; Landsiedel, R. Comparative inhalation toxicity of multi-wall carbon nanotubes, graphene, graphite nanoplatelets and low surface carbon black. *Part. Fibre Toxicol.* **2013**, *10*, 2310.1186/1743-8977-10-23

(19) Wohlleben, W.; Brill, S.; Meier, M.; Mertler, M.; Cox, G.; Hirth, S.; von Vacano, B.; Strauss, V.; Treumann, S.; Wiench, K.; Ma-Hock, L.; Landsiedel, R. On the lifecycle of nanocomposites: comparing released fragments and their in-vivo hazards from three release mechanisms and four nanocomposites. *Small* **2011**, *7*, 2384–2395.

(20) Wohlleben, W.; Kingston, C.; Carter, J.; Sahle-Demessie, E.; Vázquez-Campos, S.; Acrey, B.; Chen, C.-Y.; Walton, E.; Egenolf, H.; Müller, P.; Zepp, R. NanoRelease: Pilot interlaboratory comparison of a weathering protocol applied to resilient and labile polymers with and without embedded carbon nanotubes. *Carbon* **2017**, *113*, 346–360.

(21) Wohlleben, W.; Neubauer, N. Quantitative rates of release from weathered nanocomposites are determined across 5 orders of magnitude by the matrix, modulated by the embedded nanomaterial. *NanoImpact* **2016**, *1*, 39–45.

(22) Schlagenhauf, L.; Buerki-Thurnherr, T.; Kuo, Y.-Y.; Wichser, A.; Nüesch, F.; Wick, P.; Wang, J. Carbon Nanotubes Released from an Epoxy-Based Nanocomposite: Quantification and Particle Toxicity. *Environ. Sci. Technol.* **2015**, *49* (17), 10616–10623.

(23) OECD. Acute Toxicity Test (Annex 2 Composition of the recommended reconstituted water). *Guidelines for Testing of Chemicals*; OECD: Paris, France, **1992**, vol 203.

(24) Bicho, R. C.; Santos, F. C.; Gonçalves, M. F.; Soares, A. M.; Amorim, M. J. Enchytraeid Reproduction TestPLUS: hatching, growth and full life cycle test—an optional multi-endpoint test with *Enchytraeus crypticus*. *Ecotoxicology* **2015**, *24* (5), 1053–1063.

(25) OECD. *Guidance on Sample Preparation and Dosimetry for the Safety Testing of Manufactured Nanomaterials*; OECD: Paris, France, **2012**.

(26) Bicho, R. C.; Ribeiro, T.; Rodrigues, N. P.; Scott-Fordsmand, J. J.; Amorim, M. J. Effects of Ag nanomaterials (NM300K) and Ag salt (AgNO₃) can be discriminated in a full life cycle long term test with *Enchytraeus crypticus*. *J. Hazard. Mater.* **2016**, *318*, 608–614.

(27) Petersen, E. J.; Diamond, S. A.; Kennedy, A. J.; Goss, G. G.; Ho, K.; Lead, J.; Hanna, S. K.; Hartmann, N. B.; Hund-Rinke, K.; Mader, B.; Manier, N.; Pandard, P.; Salinas, E. R.; Sayre, P. Adapting OECD Aquatic Toxicity Tests for Use with Manufactured Nanomaterials: Key Issues and Consensus Recommendations. *Environ. Sci. Technol.* **2015**, *49* (16), 9532–9547.

(28) Lin, S.; Zhao, Y.; Ji, Z.; Ear, J.; Chang, C. H.; Zhang, H.; Low-Kam, C.; Yamada, K.; Meng, H.; Wang, X.; et al. Zebrafish high-throughput screening to study the impact of dissolvable metal oxide nanoparticles on the hatching enzyme, ZHE1. *Small* **2013**, *9* (9–10), 1776–1785.

(29) Lin, S.; Zhao, Y.; Xia, T.; Meng, H.; Ji, Z.; Liu, R.; George, S.; Xiong, S.; Wang, X.; Zhang, H.; et al. High content screening in zebrafish speeds up hazard ranking of transition metal oxide nanoparticles. *ACS Nano* **2011**, *5* (9), 7284–7295.

(30) Lin, S.; Wang, X.; Ji, Z.; Chang, C. H.; Dong, Y.; Meng, H.; Liao, Y.-P.; Wang, M.; Song, T.-B.; Kohan, S.; et al. Aspect ratio plays a role in the hazard potential of CeO₂ nanoparticles in mouse lung and zebrafish gastrointestinal tract. *ACS Nano* **2014**, *8* (5), 4450–4464.

(31) Lee, L. E.; Clemons, J. H.; Bechtel, D. G.; Caldwell, S. J.; Han, K.-B.; Pasitschniak-Arts, M.; Mosser, D. D.; Bols, N. C. Development and characterization of a rainbow trout liver cell line expressing cytochrome P450-dependent monooxygenase activity. *Cell Biol. Toxicol.* **1993**, *9* (3), 279–294.

(32) Faisal, M.; Ahne, W. A cell line (CLC) of adherent peripheral blood mononuclear leucocytes of normal common carp *Cyprinus carpio*. *Dev. Comp. Immunol.* **1990**, *14* (2), 255–260.

(33) Weyts, F.; Rombout, J.; Flik, G.; Verburg-Van Kemenade, B. A common carp (*Cyprinus carpio*L.) leucocyte cell line shares morphological and functional characteristics with macrophages. *Fish Shellfish Immunol.* **1997**, *7* (2), 123–133.

(34) Lammel, T.; Boisseaux, P.; Fernández-Cruz, M.-L.; Navas, J. M. Internalization and cytotoxicity of graphene oxide and carboxyl graphene nanoplatelets in the human hepatocellular carcinoma cell line Hep G2. *Part. Fibre Toxicol.* **2013**, *10* (1), 27.

(35) Lammel, T.; Navas, J. M. Graphene nanoplatelets spontaneously translocate into the cytosol and physically interact with cellular organelles in the fish cell line PLHC-1. *Aquat. Toxicol.* **2014**, *150*, 55–65.

(36) Schlagenhauf, L.; Kuo, Y.-Y.; Bahk, Y. K.; Nüesch, F.; Wang, J. Decomposition and particle release of a carbon nanotube/epoxy nanocomposite at elevated temperatures. *J. Nanopart. Res.* **2015**, *17* (11), 1–11.

(37) Singh, D.; Schiffman, L. A.; Watson-Wright, C.; Sotiriou, G. A.; Oyanedel-Craver, V.; Wohlleben, W.; Demokritou, P. Nanofiller presence enhances polycyclic aromatic hydrocarbon (PAH) profile on nanoparticles released during thermal decomposition of nano-enabled thermoplastics: Potential Environmental Health Implications. *Environ. Sci. Technol.* **2017**.51522210.1021/acs.est.6b06448

(38) Sotiriou, G. A.; Singh, D.; Zhang, F.; Chalbot, M.-C. G.; Spielman-Sun, E.; Hoering, L.; Kavouras, I. G.; Lowry, G. V.; Wohlleben, W.; Demokritou, P. Thermal decomposition of nano-enabled thermoplastics: Possible environmental health and safety implications. *J. Hazard. Mater.* **2016**, *305*, 87–95.

(39) Hirth, S.; Cena, L. G.; Cox, G.; Tomovic, Z.; Peters, T. M.; Wohlleben, W. Scenarios and methods that induce protruding or released CNTs after degradation of composite materials. *J. Nanopart. Res.* **2013**, *15*, 1504.

(40) Kang, J.; Erdely, A.; Afshari, A.; Casuccio, G.; Bunker, K.; Lersch, T.; Dahm, M.; Farcas, D.; Cena, L. Generation and characterization of aerosols released from sanding composite nanomaterials containing carbon nanotubes. *NanoImpact* **2017**, *5*, 41.

(41) Watson, C.; DeLoid, G.; Pal, A.; Demokritou, P. Buoyant Nanoparticles: Implications for Nano-Biointeractions in Cellular Studies. *Small* **2016**, *12*, 3172.

(42) Watson-Wright, C.; Singh, D.; Demokritou, P. Toxicological implications of released particulate matter during thermal decomposition of nano-enabled thermoplastics. *NanoImpact* **2017**, *5*, 29.

(43) Santos, F. C.; Gomes, S. I.; Scott-Fordsmand, J. J.; Amorim, M. J. Hazard assessment of Nickel nanoparticles in soil - the use of a full life cycle test with *Enchytraeus crypticus*. *Environ. Toxicol. Chem.* **2017**, *36*, 2934.

(44) Scott-Fordsmand, J. J.; Navas, J. M.; Hund-Rinke, K.; Nowack, B.; Amorim, M. J. B. Nanomaterials to microplastics: Swings and roundabouts. *Nano Today* **2017**, *17*, 7.

(45) Störmer, A.; Bott, J.; Kemmer, D.; Franz, R. Critical review of the migration potential of nanoparticles in food contact plastics. *Trends Food Sci. Technol.* **2017**, *63*, 39–50.

(46) Sussarellu, R.; Suquet, M.; Thomas, Y.; Lambert, C.; Fabioux, C.; Pernet, M. E. J.; Le Gôic, N.; Quillien, V.; Mingant, C.; Epelboin, Y.; Corporeau, C.; Guyomarch, J.; Robbens, J.; Paul-Pont, I.; Soudant, P.; Huvet, A. Oyster reproduction is affected by exposure to polystyrene microplastics. *Proc. Natl. Acad. Sci. U. S. A.* **2016**, *113* (9), 2430–2435.

(47) Avio, C. G.; Gorbi, S.; Milan, M.; Benedetti, M.; Fattorini, D.; d'Errico, G.; Pauletto, M.; Bargelloni, L.; Regoli, F. Pollutants bioavailability and toxicological risk from microplastics to marine mussels. *Environ. Pollut.* **2015**, *198*, 211–222.

(48) Ging, J.; Tejerina-Anton, R.; Ramakrishnan, G.; Nielsen, M.; Murphy, K.; Gorham, J. M.; Nguyen, T.; Orlov, A. Development of a conceptual framework for evaluation of nanomaterials release from nanocomposites: Environmental and toxicological implications. *Sci. Total Environ.* **2014**, *473*, 9–19.

(49) Gomez, V.; Levin, M.; Saber, A. T.; Irusta, S.; Dal Maso, M.; Hanoi, R.; Santamaria, J.; Jensen, K. A.; Wallin, H.; Koponen, I. K. Comparison of Dust Release from Epoxy and Paint Nanocomposites and Conventional Products during Sanding and Sawing. *Ann. Occup. Hyg.* **2014**, *58* (8), 983.

(50) Saber, A.; Koponen, I.; Jensen, K.; Jacobsen, N.; Mikkelsen, L.; Moller, P.; Loft, S.; Vogel, U.; Wallin, H. Inflammatory and genotoxic

effects of sanding dust generated from nanoparticle-containing paints and lacquers. *Nanotoxicology* **2012**, *6*, 776–788.

(51) Saber, A.; Jacobsen, N.; Mortensen, A.; Szarek, J.; Jackson, P.; Madsen, A.; Jensen, K.; Koponen, I.; Brunborg, G.; Gutzkow, K.; Vogel, U.; Wallin, H. Nanotitanium dioxide toxicity in mouse lung is reduced in sanding dust from paint. *Part. Fibre Toxicol.* **2012**, *9* (1), 4.

(52) Wohlleben, W.; Meier, M. W.; Vogel, S.; Landsiedel, R.; Cox, G.; Hirth, S.; Tomović, Ž. Elastic CNT–polyurethane nanocomposite: synthesis, performance and assessment of fragments released during use. *Nanoscale* **2013**, *5* (1), 369–380.

(53) Saber, A. T.; Mortensen, A.; Szarek, J.; Koponen, I. K.; Levin, M.; Jacobsen, N. R.; Pozzebon, M. E.; Mucelli, S. P.; Rickerby, D. G.; Kling, K.; et al. Epoxy composite dusts with and without carbon nanotubes cause similar pulmonary responses, but differences in liver histology in mice following pulmonary deposition. *Part. Fibre Toxicol.* **2015**, *13* (1), 1–20.

(54) Kaiser, J. P.; Roesslein, M.; Diener, L.; Wick, P. Human Health Risk of Ingested Nanoparticles That Are Added as Multifunctional Agents to Paints: an In Vitro Study. *PLoS One* **2013**, *8* (12), e83215.

(55) Semenzin, E.; Hristozov, D.; Caballero, A.; Scott-Fordsmand, J.; Gottschalk, F.; Basei, G. P.; Subramanian, V.; Zabeo, A.; Nowack, B.; Marcomini, A. Ecological risk along the life-cycle of nano-enabled products. *In preparation* **2017**.

(56) Pillai, K. V.; Gray, P. J.; Tien, C.-C.; Bleher, R.; Sung, L.-P.; Duncan, T. V. Environmental release of core-shell semiconductor nanocrystals from free-standing polymer nanocomposite films. *Environ. Sci.: Nano* **2016**, *3* (3), 657–669.

(57) Mitrano, D. M.; Mehrabi, K.; Arroyo, Y.; Nowack, B. Mobility of metallic (nano)particles in leachates from landfills containing waste incineration residues. *Environmental Science: Nano* **2016**, No. 2, 1.

(58) Mitrano, D. M.; Limpitprakan, P.; Babel, S.; Nowack, B. Durability of nano-enhanced textiles through the life cycle: releases from landfilling after washing. *Environ. Sci.: Nano* **2016**, *3* (2), 375–387.

(59) Wohlleben, W.; Meyer, J.; Müller, J.; Müller, P.; Vilsmeier, K.; Stahlmecke, B.; Kuhlbusch, T. A. J. Release from nanomaterials during their use phase: combined mechanical and chemical stresses applied to simple and multi-filler nanocomposites mimicking wear of nano-reinforced tires. *Environ. Sci.: Nano* **2016**, *3*, 1036–1051.

(60) Lassen, C.; Hansen, S. F.; Magnusson, K.; Norèn, F.; Bloch Hartmann, N. I.; Jensen, P. R.; Nielsen, T. G.; Brinch, A.; *Microplastics - Occurrence, effects and sources of releases to the environment in Denmark*; Ministry of Environment and Food Denmark, Copenhagen: 2015, pp 1–205; accessible at <http://mst.dk/service/publikationer/publikation-sarkiv/2015/nov/rapport-om-mikroplast/>.

(61) Taylor, M. L.; Gwinnett, C.; Robinson, L. F.; Woodall, L. C. Plastic microfibre ingestion by deep-sea organisms. *Sci. Rep.* **2016**, *6*, 33997.

(62) Deng, Y.; Zhang, Y.; Lemos, B.; Ren, H. Tissue accumulation of microplastics in mice and biomarker responses suggest widespread health risks of exposure. *Sci. Rep.* **2017**, *7*, 46687.